Supplementary Information:
A competitive complex formation mechanism underlies trichome patterning on *Arabidopsis* leaves

Simona Digiuni, Swen Schellmann, Florian Geier, Bettina Greese, Martina Pesch, Katja Wester, Burcu Dartan, Valerie Mach, Bhylahalli Purushottam Srinivas, Jens Timmer, Christian Fleck and Martin Hülskamp

Contents

1 Linear Stability Analysis

In the main text, we present the results of a linear stability analysis that we perform in order to determine whether our model is able to form patterns from uniform conditions given a particular parameter set. Here, additional details are given to enable the readers to follow the main steps of the analysis.
Our trichome patterning model forms patterns if the inhibitor TRY acts non-cell autonomously, i.e., if the passive transport of the inhibitor TRY is included. This pattern forming ability is a special case of the general concept of a Turing instability. A Turing instability arises if a model without cellular interactions has a uniform stable steady state, i.e., all cells have identical species concentrations, which becomes unstable in the presence of cellular interactions[1,2]. Usually the initial instability will be bounded by non-linear feedback regulations such that the deviations from the uniform steady state will eventually weaken and a new non-uniform steady state, i.e., a spatial pattern, is formed. The analysis of a Turing instability proceeds in two steps. First, the stability of the uniform steady state is verified by means of a linear stability analysis. This means it is investigated whether small uniform deviations form the uniform steady state will decay with time. This is identical to the investigation of a single cell model as the spatical coupling term eqn. (6) vanishes in this case. Second, the coupling between cells is included and the stability of the uniform steady state in the presence of variations between different cells is analysed. This is again performed by means of a linear stability analysis. To facilitate the analysis the inter-cellular variations are represented in a discrete Fourier space.
In the following three sections we first present our trichome patterning model, then analyse a single cell version of the model and give conditions for the stability of a particular steady state. Finally, we analyse the multi-cellular system and determine conditions which must be violated in order to form spatial patterns.

1.1 Trichome patterning model

We start with our dimensionless model for trichome pattering as presented in the Materials and Methods section of the main text. It consists of the following system of coupled differential equations:

$$\partial_\tau [gl1]_j = k_1 + k_2[ac]_j - [gl1]_j(1 + [gl3]_j + k_3[try]_j) \tag{1}$$
$$\partial_\tau [gl3]_j = k_4 + k_5[ac]_j - [gl3]_j(k_6 + [gl1]_j + k_7[try]_j) + k_6k_8\langle[gl3]_j\rangle \tag{2}$$
$$\partial_\tau [try]_j = k_9 + k_{10}[ac]_j^2 - [try]_j(k_{11} + k_3[gl1]_j + k_7[gl3]_j + k_{12}[ac]_j) + k_{11}k_{13}\langle[try]_j\rangle \tag{3}$$
$$\partial_\tau [ac]_j = [gl1]_j[gl3]_j - [ac]_j(k_{14} + k_{12}[try]_j), \tag{4}$$

where the coupling term is defined as

$$\langle[c]_{x,y}\rangle = [c]_{x-1,y} + [c]_{x+1,y} + [c]_{x,y-1} + [c]_{x,y+1} + [c]_{x+1,y-1} + [c]_{x-1,y+1} - 6[c]_{x,y}. \tag{5}$$

For ease of notation, we introduce a column vector $\mathbf{v}$ with all four substances as its elements, i.e., $\mathbf{v} = ([gl1], [gl3], [try], [ac])^T$, and rewrite the system of eqns. (1-4) as one equation:

$$\partial_\tau \mathbf{v}_j = \mathbf{f}\left(\mathbf{v}_j\right) + \mathbf{D} \cdot \langle \mathbf{v}_j \rangle \tag{6}$$

with $\mathbf{f}(\mathbf{v}) = (f_1(\mathbf{v}), f_2(\mathbf{v}), f_3(\mathbf{v}), f_4(\mathbf{v}))^T$, and $\mathbf{D} = \text{diag}\,(0, k_6k_8, k_{11}k_{13}, 0)^T$. In our case, the reaction functions are

$$\begin{aligned}
f_1(\mathbf{v}) =& k_1 + k_2[ac]_j - [gl1]_j(1 + [gl3]_j + k_3[try]_j) \\
f_2(\mathbf{v}) =& k_4 + k_5[ac]_j - [gl3]_j(k_6 + [gl1]_j + k_7[try]_j) \\
f_3(\mathbf{v}) =& k_9 + k_{10}[ac]_j^2 - [try]_j(k_{11} + k_3[gl1]_j + k_7[gl3]_j + k_{12}[ac]_j) \\
f_4(\mathbf{v}) =& [gl1]_j[gl3]_j - [ac]_j(k_{14} + k_{12}[try]_j).
\end{aligned}$$

1.2 Steady state analysis of the single cell model

In order to find a uniform steady state $\mathbf{v}_0$ of the system of eqns. (1-4) without transport (i.e., $\mathbf{D} = \mathbf{0}$), we solve the system $\mathbf{f}(\mathbf{v}_0) = \mathbf{0}$. We aim to determine the stability of this steady state by looking at the evolution of small perturbations from the steady state, i.e., $\bar{\mathbf{v}} = \mathbf{v} - \mathbf{v}_0$. To see if these perturbations grow or decay with time, we substitute them into the differential eqn. (6) and apply a Taylor series expansion of $\mathbf{f}$ around the steady state $\mathbf{v}_0$, i.e.,

$$\mathbf{f}(\mathbf{v}_0 + \bar{\mathbf{v}}) = \mathbf{f}(\mathbf{v}_0) + \mathbf{J}_0 \cdot \bar{\mathbf{v}} + O\left(|\bar{\mathbf{v}}|^2\right).$$

Since we look at small perturbations we neglect the higher order terms $O\left(|\bar{\mathbf{v}}|^2\right)$ and arrive at a linear ordinary differential equation for the perturbations $\bar{\mathbf{v}}$:

$$\partial_\tau \bar{\mathbf{v}} = \mathbf{J}_0 \cdot \bar{\mathbf{v}}. \tag{7}$$

Here, the Jacobian matrix $\mathbf{J}_0$ is the matrix of partial derivatives $J_{i,k} = \partial f_i / \partial v_k$, evaluated at the steady state $\mathbf{v}_0$. In our case it has the form

$$\mathbf{J}_0 = \begin{pmatrix} -1-[gl3]-k_3[try] & -[gl1] & -k_3[gl1] & k_2 \\ -[gl3] & -k_6-[gl1]-k_7[try] & -k_7[gl3] & k_5 \\ -k_3[try] & -k_7[try] & -k_{11}-k_3[gl1]-k_7[gl3]-k_{12}[ac] & 2k_{10}[ac]-k_{12}[try] \\ [gl3] & [gl1] & -k_{12}[ac] & -k_{14}-k_{12}[try] \end{pmatrix}.$$

The general solution of eqn. (7) is

$$\bar{\mathbf{v}}(\tau) = \sum_{n=1}^{4} u_n e^{\lambda_n \tau} \mathbf{w}_n, \tag{8}$$

where the constants u_n are set by the initial conditions, $\mathbf{w}_n$ are the normalized eigenvectors and λ_n are the eigenvalues of the Jacobian matrix $\mathbf{J}_0$ evaluated at the steady state $\mathbf{v}_0$. The steady state is stable if the perturbations $\bar{\mathbf{v}}$ decay with time, which is equivalent to the statement that all eigenvalues λ_n have negative real parts. The eigenvalues λ_n are the solutions of the equation

$$\det(\mathbf{J}_0 - \lambda \mathbf{I}) = 0,$$

where $\mathbf{I}$ is the identity matrix, i.e. $\mathbf{I} = \mathrm{diag}(1, 1, 1, 1)$. Evaluating the determinant results in a characteristic equation of the form

$$\lambda^4 + a_1\lambda^3 + a_2\lambda^2 + a_3\lambda + a_4 = 0. \tag{9}$$

As we are only interested in the quality (i.e., real vs. complex, positive vs. negative) of the eigenvalues, we do not have to explicitly calculate them. Instead, we use the Routh-Hurwitz criteria, which are necessary and sufficient conditions that all eigenvalues have negative real parts[3]. For the coefficients of the characteristic eqn. (9), these criteria are

$$a_1 > 0, \quad a_3 > 0, \quad a_4 > 0, \quad a_1 a_2 a_3 > a_3^2 + a_1^2 a_4. \tag{10}$$

As we could not obtain an analyical expression for the steady state of our system of eqns. (1-4), we cannot give a full parameteric representation of these coefficients. For the model analysis we determine the steady states by numerical integration, starting with zero initial conditions for all protein concentrations. This approach assumes that the system is in a homogeneous steady state before cellular coupling becomes important. Given the numerically determined steady state, the coefficients are,

$$\begin{aligned} a_1 &= 1 + [gl1] + [gl3] + k_{11} + [ac]k_{12} + k_{14} + [gl1]k_3 + k_6 + [gl3]k_7 + (k_{12} + k_3 + k_7)[try] \\ a_2 &= k_{11} + [ac]k_{12} + 2[ac]^2 k_{10} k_{12} + k_{14} + [ac]k_{12}k_{14} + [gl1]^2 k3 + k_6 + [ac]k_{12}k_6 \\ &\quad + k_{14}k_6 + k_{11}(k_{14} + k_6) + [gl3]^2 k_7 + (k_3(k_{11} + k_{14} + k_6) + (1 + k_{11} + k_{14})k_7 \\ &\quad + k_{12}(1 + k_{11} + k_6 + [ac](k_3 + k_7)))[try] + (k_3 k_7 + k_{12}(k_3 + k_7))[try]^2 \\ &\quad + [gl1](1 + k_{11} + [ac]k_{12} + k_{14} + k_3 + [gl3]k_3 + k_{14}k_3 - k_5 + k_3 k_6 \\ &\qquad + [gl3]k_7 + k_{12}[try] + k_3(1 + k_{12} + k_7)[try]) \\ &\quad + [gl3](k_{11} + [ac]k_{12} + k_{14} - k_2 + k_6 + (1 + k_{14} + k_6)k_7 + (k_{12} + (1 + k_{12} + k3)k_7)[try]) \end{aligned}$$

$$
\begin{aligned}
a_3 \;=\;& k_{11}k_{14} + [gl3]k_{11}k_{14} - [gl3]k_{11}k_2 + k_{11}k_6 + [gl3]k_{11}k_6 + k_{14}k_6 \\
&+[gl3]k_{14}k_6 + k_{11}k_{14}k_6 - [gl3]k_2k_6 + [gl3]k_{14}k_7 + [gl3]^2k_{14}k_7 - [gl3]^2k_2k_7 \\
&+[gl3]k_6k_7 + [gl3]^2k_6k_7 + [gl3]k_{14}k_6k_7 \\
&+((k_{12} + [gl3]k_{12} + k_{14}k_3)k_6 \\
&\quad +(k_{14} + [gl3](k_{14} - k_2 + k_{14}k_3 + k_3k_6 + k_{12}(1 + [gl3] + k_6)))k_7 \\
&\quad +k_{11}(k_{12}(1 + [gl3] + k_6) + k_3(k_{14} + k_6) + (1 + [gl3] + k_{14})k_7))[try] \\
&+(k_{12}k_3(k_{11} + k_6) + ((k_{11} + k_{14})k_3 + k_{12}(1 + [gl3] + k_{11} + [gl3]k_3))k_7)[try]^2 \\
&+k_{12}k_3k_7[try]^3 + [gl1]^2k_3(1 + k_{14} - k_5 + k_{12}[try]) \\
&+2[ac]^2k_{10}k_{12}(1 + [gl3] + k_6 + (k_3 + k_7)[try]) \\
&+[gl1](2[ac]^2k_{10}k_{12} + k_{14} + k_{14}k_3 + [gl3]k_{14}k_3 - [gl3]k_2k_3 - k_5 + k_3k_6 \\
&\qquad +[gl3]k_3k_6 + k_{14}k_3k_6 + [gl3]k_7 + [gl3]k_{14}k_7 - [gl3]k_5k_7 + k_{12}[try] \\
&\qquad +k_3(k_{12} + k_{14} - k_5 + k_{12}k_6 + k_7 + 4[gl3]k_7 + k_{14}k_7)[try] + k_{12}k_3(1 + k_7)[try]^2 \\
&\qquad +k_{11}(1 + k_{14} - k_5 + (k_{12} + k_3)[try]) + [ac](2[gl3]k_{10}(k_3 + k_7) \\
&\qquad +k_{12}(1 + k_{14} - k_5 + k_3[try]))) \\
&+[ac]k_{12}(k_6 + [gl3](k_6 - k_2 + k_7[try]) + k_{14}(1 + [gl3] + k_6 + (k_3 + k_7)[try]) \\
&\qquad +[try](k_7 - k_5k_7 + k_3(k_6 - k_2 + k_7[try])))
\end{aligned}
$$

$$
\begin{aligned}
a_4 \;=\;& [gl1]^2k_3(k_{14} - k_5 + k_{12}[try]) \\
&+[gl1](k_{14}k_3k_6 + [gl3]k_{14}k_3k_6 - [gl3]k_2k_3k_6 + [gl3]k_{14}k_7 - [gl3]k_5k_7 \\
&\qquad +k_3(k_{12}k_6 + (k_{14} + 4[gl3]k_{14} - 2[gl3](k_2 + k_5))k_7)[try] + (1 + 2[gl3])k_{12}k_3k_7[try]^2 \\
&\qquad +k_{11}(k_{14} - k_5 + k_{12}[try])(1 + k_3[try])) \\
&+((1 + [gl3])k_{12}[try] - [gl3]k_2 + k_{12}k_3[try]^2 + k_{14}(1 + [gl3] + k_3[try])) \\
&\times([gl3]k_6k_7 + k_{11}(k_6 + k_7[try])) \\
&+2[ac]^2k_{10}k_{12}([gl1] + [gl1]k3[try] + (1 + [gl3] + k_3[try])(k_6 + k_7[try])) \\
&+[ac](k_{12}(k_{14}(1 + [gl3] + k_3[try])(k_6 + k_7[try]) - [gl3](k_2k_6 + k_5k_7[try]) \\
&\qquad -[try](k_2k_3k_6 + k_5k_7 + k_3(k_2 + k_5)k_7[try])) \\
&\qquad +[gl1](k_{12}(k_{14} - k_5 + (k_{14} - k_2)k_3[try]) + 2[gl3]k_{10}(k_7 + k_3(k_6 + 2k_7[try])))).
\end{aligned}
$$

1.3 Steady state analysis of the multi-cellular model

In the next step, we consider the model including cellular coupling, i.e., including transport of TRY. The stability of the uniform steady state with respect to variations in the concentration between different cells, i.e., $\bar{\mathbf{v}}_j = \mathbf{v}_j - \mathbf{v}_0$ is again investigated by means of a linear stability analysis. Applying a linearization of eqns. (1-4) we arrive at a system of $4 \cdot x_{max} \cdot y_{max}$ coupled linear ODEs, i.e.,

$$\partial_\tau \bar{\mathbf{v}}_j = \mathbf{J}_0 \cdot \bar{\mathbf{v}}_j + \mathbf{D} \cdot \langle \bar{\mathbf{v}}_j \rangle, \tag{11}$$

In order to decouple the system of eqn. (11), we apply a discrete Fourier transformation. In other words, we look for periodic solutions of the form

$$\bar{\mathbf{v}}_j = \bar{\mathbf{v}}_{x,y} = \sum_{s=1}^{x_{max}} \sum_{r=1}^{y_{max}} \boldsymbol{\nu}_{s,r} \; e^{\frac{2\pi i s x}{x_{max}}} \; e^{\frac{2\pi i r y}{y_{max}}}. \tag{12}$$

Note that the time-dependent coefficients $\boldsymbol{\nu}_{s,r}$ play the role of amplitudes of a two-dimensional periodic pattern. In analogy to eqn. (12), where the spatial variations are expressed in terms of amplitudes, we can also express the amplitudes in terms of the spatial variations. This is illustrated in the following

calculations. Multiplying eqn. (12) by $e^{-2\pi ipx/x_{max}} e^{-2\pi iqy/y_{max}}$ and summing each side over $1 \le x \le x_{max}$ and $1 \le y \le y_{max}$ yields

$$\sum_{x=1}^{x_{max}} \sum_{y=1}^{y_{max}} \bar{\mathbf{v}}_{x,y} \; e^{-2\pi ipx/x_{max}} e^{-2\pi iqy/y_{max}} = \sum_{x=1}^{x_{max}} \sum_{y=1}^{y_{max}} \sum_{s=1}^{x_{max}} \sum_{r=1}^{y_{max}} \boldsymbol{\nu}_{s,r} \; e^{\frac{2\pi isx}{x_{max}}} \; e^{\frac{2\pi iry}{y_{max}}} \; e^{-\frac{2\pi ipx}{x_{max}}} \; e^{-\frac{2\pi iqy}{y_{max}}}$$

$$= \sum_{s=1}^{x_{max}} \sum_{r=1}^{y_{max}} \boldsymbol{\nu}_{s,r} \left(\sum_{x=1}^{x_{max}} e^{\frac{2\pi i(s-p)x}{x_{max}}} \right) \left(\sum_{y=1}^{y_{max}} e^{\frac{2\pi i(r-q)y}{y_{max}}} \right). \tag{13}$$

The two factors in brackets are simplified considerably by the formulas

$$\sum_{x=1}^{x_{max}} e^{\frac{2\pi i(s-p)x}{x_{max}}} = x_{max} \delta_{s,p} \tag{14}$$

$$\sum_{y=1}^{y_{max}} e^{\frac{2\pi i(r-q)y}{y_{max}}} = y_{max} \delta_{r,q} \tag{15}$$

with the Kronecker delta $\delta_{s,p}$ defined by

$$\delta_{s,p} = \begin{cases} 1 & \text{for} \quad s = p \\ 0 & \text{for} \quad s \neq p. \end{cases}$$

Substituting eqns. (14-15) into eqn. (13), we get

$$\sum_{x=1}^{x_{max}} \sum_{y=1}^{y_{max}} \bar{\mathbf{v}}_{x,y} \; e^{-2\pi ipx/x_{max}} e^{-2\pi iqy/y_{max}} = \sum_{s=1}^{x_{max}} \sum_{r=1}^{y_{max}} \boldsymbol{\nu}_{s,r} \; x_{max} \delta_{s,p} \; y_{max} \delta_{r,q} = \boldsymbol{\nu}_{p,q} x_{max} y_{max}. \tag{16}$$

Dividing by $x_{max} y_{max}$ gives the amplitude equations mentioned above. Before we make use of this result, we first need to express the spatial coupling in terms of the amplitudes $\boldsymbol{\nu}_{s,r}$. We apply the Fourier transformation eqn. (12) to $\langle [\mathbf{v}]_{x,y} \rangle$ (defined in analogy to eqn. (5)) and obtain

$$\langle [\mathbf{v}]_{x,y} \rangle = \sum_{s=1}^{x_{max}} \sum_{r=1}^{y_{max}} \boldsymbol{\nu}_{s,r} \; e^{\frac{2\pi isx}{x_{max}}} e^{\frac{2\pi iry}{y_{max}}} \left(e^{\frac{-2\pi is}{x_{max}}} + e^{\frac{2\pi is}{x_{max}}} + e^{\frac{-2\pi ir}{y_{max}}} + e^{\frac{2\pi ir}{y_{max}}} + e^{\frac{2\pi is}{x_{max}}} e^{\frac{-2\pi ir}{y_{max}}} + e^{\frac{-2\pi is}{x_{max}}} e^{\frac{2\pi ir}{y_{max}}} - 6 \right)$$

$$= - \sum_{s=1}^{x_{max}} \sum_{r=1}^{y_{max}} \boldsymbol{\nu}_{s,r} \; e^{\frac{2\pi isx}{x_{max}}} e^{\frac{2\pi iry}{y_{max}}} \cdot d_{p,q} \tag{17}$$

where

$$d_{p,q} = 4 \left[\sin^2 \left(\frac{\pi p}{x_{max}} \right) + \sin^2 \left(\frac{\pi q}{y_{max}} \right) + \sin^2 \left(\frac{\pi p}{x_{max}} - \frac{\pi q}{y_{max}} \right) \right].$$

The last expression is derived using the fact that

$$\sin(\phi) = \frac{1}{2i} \left(e^{i\phi} - e^{-i\phi} \right) \Rightarrow \sin^2(\phi) = - \frac{1}{4} \left(e^{2i\phi} + e^{-2i\phi} - 2 \right).$$

Applying the same procedure as above leads to

$$\sum_{x=1}^{x_{max}} \sum_{y=1}^{y_{max}} \langle [\mathbf{v}]_{x,y} \rangle e^{-2\pi ipx/x_{max}} e^{-2\pi iqy/y_{max}} = -\boldsymbol{\nu}_{p,q} x_{max} y_{max} d_{p,q}, \tag{18}$$

Finally, we transform the linearization of the coupled system. Here, we first multiply eqn. (7) by $e^{-2\pi ipx/x_{max}} e^{-2\pi iqy/y_{max}}$, sum over $1 \le x \le x_{max}$ and $1 \le y \le y_{max}$, and rearrange. This yields

$$\partial_\tau \sum_{x=1}^{x_{max}} \sum_{y=1}^{y_{max}} \bar{\mathbf{v}}_j \; e^{\frac{-2\pi isx}{x_{max}}} \; e^{\frac{-2\pi iry}{y_{max}}} = \mathbf{J}_0 \cdot \sum_{x=1}^{x_{max}} \sum_{y=1}^{y_{max}} \bar{\mathbf{v}}_j \; e^{\frac{-2\pi isx}{x_{max}}} \; e^{\frac{-2\pi iry}{y_{max}}} + \mathbf{D} \cdot \sum_{x=1}^{x_{max}} \sum_{y=1}^{y_{max}} \langle \bar{\mathbf{v}}_j \rangle \; e^{\frac{-2\pi isx}{x_{max}}} \; e^{\frac{-2\pi iry}{y_{max}}}.$$

Then substituting eqn. (16) and eqn. (18) leads to the transformed linearisation of the coupled system

$$\partial_\tau \boldsymbol{\nu}_{p,q} = \mathbf{A}_{p,q} \cdot \boldsymbol{\nu}_{p,q}, \qquad \mathbf{A}_{p,q} = \mathbf{J}_0 - \mathbf{D} \cdot d_{p,q}, \tag{19}$$

with the coupling matrix

$$\mathbf{D} \cdot d_{p,q} = \begin{pmatrix} 0 & 0 & 0 & 0 \\ 0 & k_6 k_8 d_{p,q} & 0 & 0 \\ 0 & 0 & k_{11} k_{13} d_{p,q} & 0 \\ 0 & 0 & 0 & 0 \end{pmatrix}.$$

Note that the transformation leads to a decoupling of the original system of $4 \cdot x_{max} \cdot y_{max}$ equations into $x_{max} \cdot y_{max}$ sets of four equations. Each set describes the temporal evolution of the amplitude of a periodic pattern with a pair of spatial frequencies $\pi p / x_{max}$ and $\pi q / y_{max}$.
Based on a similar argument as above, the celluar variations represented by the Fourier amplitudes grow if for any given $1 \leq p \leq x_{max}$ and $1 \leq q \leq y_{max}$ the matrix $\mathbf{A}_{p,q}$ has an eigenvalue with positive real part. This is equivalent to the finding that the Routh-Hurwitz criteria are not fulfilled. Again, we first need the characteristic equation for the matrix $\mathbf{A}_{p,q}$, which is

$$\det\left(\mathbf{A}_{p,q} - \lambda \mathbf{I}\right) = 0.$$

Evaluation of this equation leads to

$$\lambda^4 + b_1(p,q)\lambda^3 + b_2(p,q)\lambda^2 + b_3(p,q)\lambda + b_4(p,q) = 0.$$

Transport-driven instability arises if at least one of the following criteria is violated:

$$\begin{aligned} b_1(p,q) > 0, \;\; b_3(p,q) > 0, \;\; b_4(p,q) > 0, \\ b_1(p,q) b_2(p,q) b_3(p,q) > b_3^2(p,q) + b_1^2(p,q) b_4(p,q). \end{aligned} \tag{20}$$

The value of these coefficients are

$$\begin{aligned} b_1(p,q) &= a_1 + D_{p,q} \\ b_2(p,q) &= a_2 + D_{p,q}(1 + [gl1] + [gl3] + k_{14} + k_6 + (k_{12} + k_3 + k_7)[try]) \\ b_3(p,q) &= a_3 + D_{p,q}([gl1] + k_{14} + [gl1]k_{14} + [gl3]k_{14} - [gl3]k_2 - [gl1]k_5 + k_6 \\ &\quad + [gl3]k_6 + k_{14}k_6 + (k_{12}(1 + [gl1] + [gl3] + k_6) + k_3([gl1] + k_{14} + k_6) \\ &\quad + (1 + [gl3] + k_{14})k_7)[try] + (k_3 k_7 + k_{12}(k_3 + k_7))[try]^2) \\ b_4(p,q) &= a_4 + D_{p,q}([gl1](k_{14} - k_5 + k_{12}[try])(1 + k_3[try]) \\ &\quad + (k_6 + k_7[try])((1 + [gl3])k_{12}[try] - [gl3]k_2 + k_{12}k_3[try]^2 \\ &\quad + k_{14}(1 + [gl3] + k_3[try]))), \end{aligned}$$

where $D_{p,q} = 4k_{11}k_{13}(\sin^2(q\pi/y_{max}) + \sin^2(p\pi/x_{max}) + \sin^2((q/y_{max} - p/x_{max})\pi))$. For our search for models with Turing instability, it is noteworthy that the coefficients $b_n(p,q)$ are linear functions of $D_{p,q}$, i.e., they are of the form $b_n(p,q) = a_n + D_{p,q}c_n$. As the a_n (by eqn. (10)) and $D_{p,q}$ are positive, the first three conditions in eqn. (20) can only be violated if the factor c_n is negative. Moreover, it is necessary and sufficient if one of them is violated at the maximum of $D_{p,q}$. In that case, the model shows pattern formation for at least one set (p,q). By numerical simulations, we found parameter samples that show transport-driven instability, i.e, fulfill all conditions in eqn. (10) and violate at least one condition of eqn. (20). In our examination, the condition $b_4(p,q) > 0$ was violated in every case.
Figures 2 H-I of the main text show the result of this numerical analysis. Regions in parameter space which show transport-driven instability are indicated in white while stable regions are given in grey.

2 References

1. Turing A M (1952) The chemical basis of morphogenesis. *Phil. Trans. R. Soc. London B* **237**, 37-72

2. Murray J D (2003) *Mathematical Biology*, Third Edition, Volume 18 of Interdisciplinary Applied Mathematics. Springer-Verlag, New York, USA

3. Edelstein-Keshet L (1988) *Mathematical Models in Biology*, Volume 46 of Classics in Applied Mathematics. SIAM, Philadelphia, USA

3 Supplementary Figures

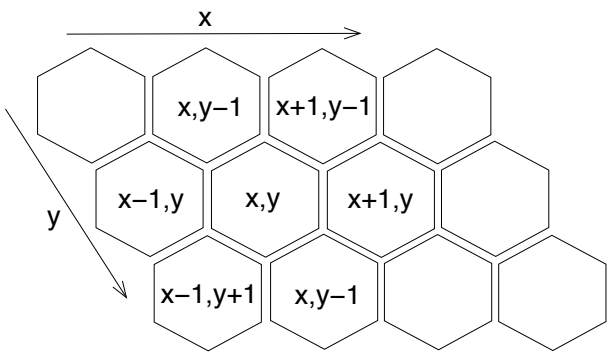

Supplementary Figure 1: **Indexing scheme of the hexagonal grid.**

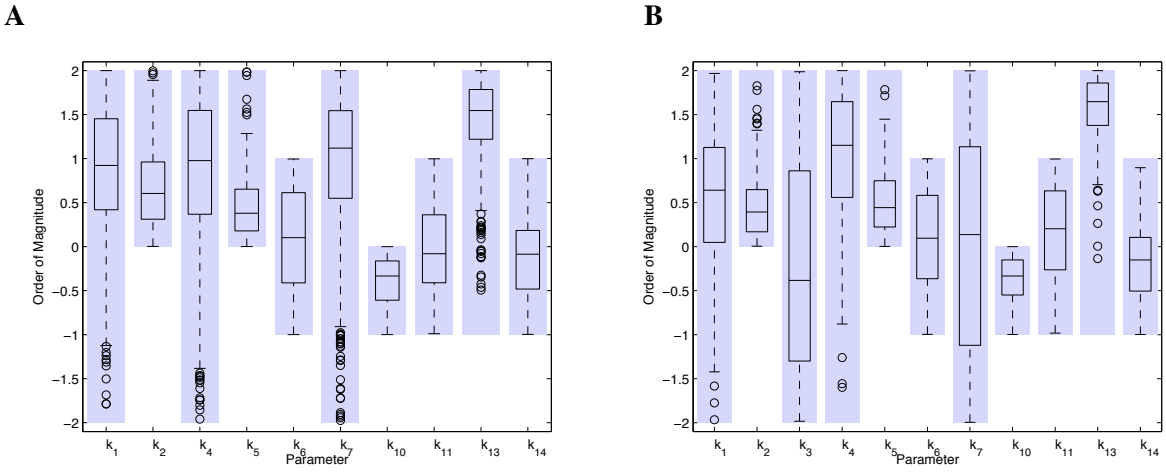

Supplementary Figure 2: **Comparison of the parameter values of the two competitive scenarios. (A)** Boxplot of the parameter values of the hits in the single competitive scenario on a logarithmic scale. The term hits refers to those randomly drawn parameter samples that fulfill all five criteria given in the main text. The box represents the values between the 25% and 75% quantiles (i.e., quartiles) with the median denoted by the central line. The whiskers delimit the range of values that lie within the 1.5 fold interquartile range, and the circles symbolize outliers. The shaded area corresponds to the range of parameter that was fixed prior to the simulations based on biological knowledge. These ranges are given in Table I in the main text. **(B)** Boxplot of the parameter values of the hits in the double competitive scenario on a logarithmic scale. See (A) for a description of the plot. Note that this boxplot contains an additional parameter, namely k_3, the relative complex formation rate of TRY and GL1. In comparison with the single competitive scenario, the median of k_7, the analogous rate for TRY and GL3, is much smaller in the double competitive scenario.

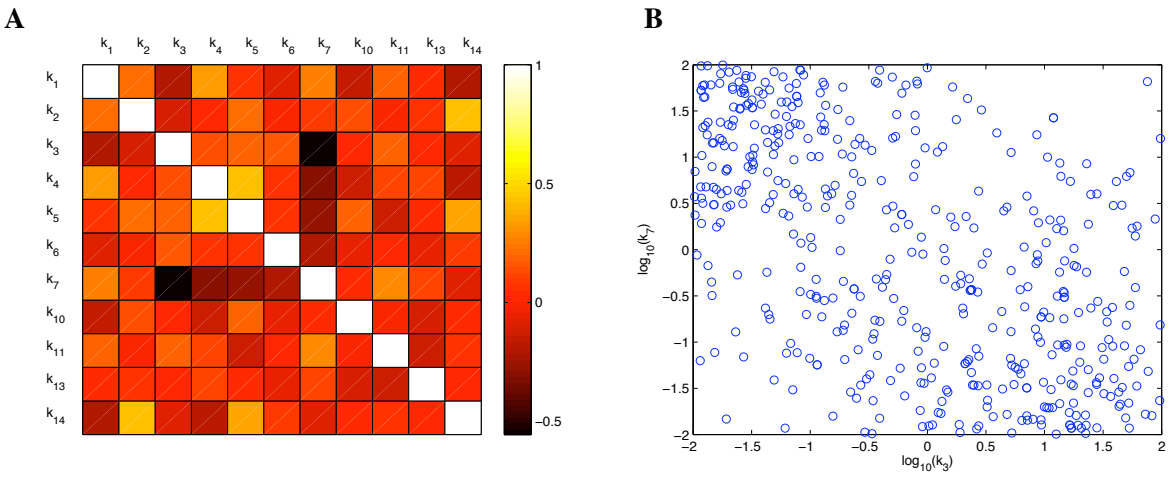

Supplementary Figure 3: **Properties of the double competitive inhibition.** **(A)** Parameter correlations of the hits in the double competitive inhibition scenario. A strong negative correlation is found between k_3, the rate of complex formation of TRY and GL1, and k_7 the rate of TRY and GL3 interaction. **(B)** Scatter plot of the k_3 and k_7 values of the hits. Note the logarithmic scale. The values accumulate in the top left and bottom right quadrant reflecting their negative correlation. These two plots illustrate that in the double competitive scenario the inhibition is primarily exerted through binding with either GL3 or GL1 reducing it to a single competitive inhibition scenario.

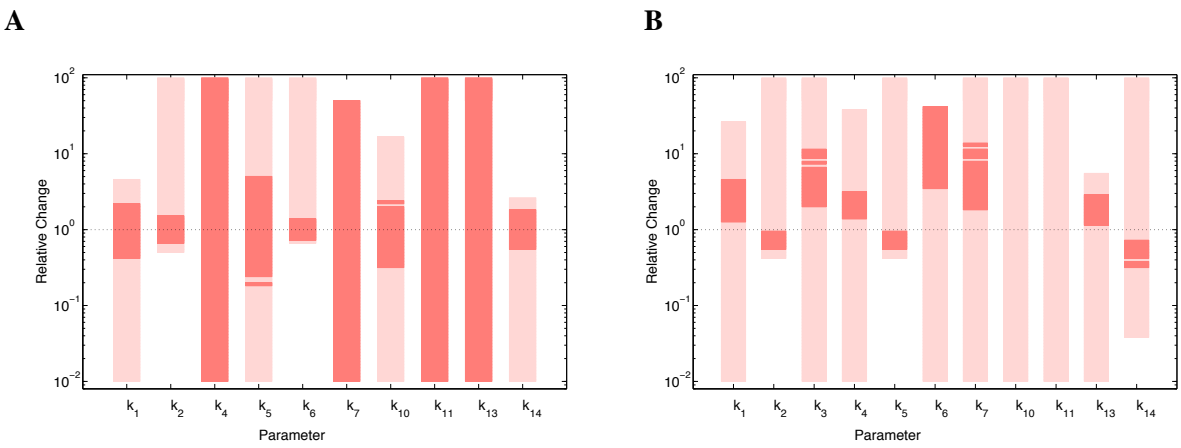

Supplementary Figure 4: **Comparison of the parameter sensitivities of the two competitive scenarios.** **(A)** Relative parameter sensitivities of the single competitive scenario. Each model parameter is changed separately over four orders of magnitude relative to its median value given in Table I of the main text. Light pink indicates whether the perturbed parameter set gives rise to a Turing instability. Dark pink indicates whether all five criteria of the over-expression experiments as defined in the main text are met. **(B)** Relative parameter sensitivities of the double competitive scenario. See (B) for a description of the plot. Note that the single competitive scenario (A) tolerates larger parameter perturbations than the double competitive scenario (B) while still fulfilling all criteria. In particular, the median parameter values of the double competitive scenario do not meet the over-expression criteria.